UC Irvine

UC Irvine Previously Published Works

Title

Video-based kinetic analysis of calcification in live osteogenic human embryonic stem cell cultures reveals the developmentally toxic effect of Snus tobacco extract

Permalink

https://escholarship.org/uc/item/0137c4b5

Authors

Martinez, Ivann KC

Sparks, Nicole RL

Madrid, Joseph V

et al.

Publication Date

2019

DOI

10.1016/j.taap.2018.11.006

Peer reviewed

eScholarship.org Powered by the California Digital Library
University of California

Author Manuscript

Author Manuscript

Author Manuscript

Author Manuscript

HHS Public Access

Author manuscript

*Toxicol Appl Pharmacol*. Author manuscript; available in PMC 2020 January 15.

Published in final edited form as:

*Toxicol Appl Pharmacol*. 2019 January 15; 363: 111–121. doi:10.1016/j.taap.2018.11.006.

# Video-based kinetic analysis of calcification in live osteogenic human embryonic stem cell cultures reveals the developmentally toxic effect of Snus tobacco extract

**Ivann K.C. Martinez**[1,2], **Nicole R.L. Sparks**[1,3], **Joseph V. Madrid**[1], **Henry Affeldt III**[1], **Madeline K.M. Vera**[1,3], **Bir Bhanu**[4], and **Nicole I. zur Nieden**[1,2,3,*]

[1]Department of Molecular, Cell & Systems Biology and Stem Cell Center, College of Natural and Agricultural Sciences, University of California Riverside, Riverside, CA, 92521, United States of America

[2]IGERT Graduate Program in Video Bioinformatics and Cell, Molecular and Developmental Biology Graduate Program, University of California Riverside, Riverside, California, United States of America

[3]Environmental Toxicology Graduate Program, University of California Riverside, Riverside, California, United States of America

[4]Center for Research in Intelligent Systems, Bourns College of Engineering, University of California Riverside, Riverside, California, United States of America

## Abstract

Epidemiological studies suggest tobacco consumption as a probable environmental factor for a variety of congenital anomalies, including low bone mass and increased fracture risk. Despite intensive public health initiatives to publicize the detrimental effects of tobacco use during pregnancy, approximately 10–20% of women in the United States still consume tobacco during pregnancy, some opting for so-called harm-reduction tobacco. These include Snus, a type of orally-consumed yet spit-free chewing tobacco, which is purported to expose users to fewer harmful chemicals. Concerns remain from a developmental health perspective since Snus has not reduced overall health risk to consumers and virtually nothing is known about whether skeletal problems from intrauterine exposure arise in the embryo.

Utilizing a newly developed video-based calcification assay we determined that extracts from Snus tobacco hindered calcification of osteoblasts derived from pluripotent stem cells early on in their differentiation. Nicotine, a major component of tobacco products, had no measurable effect in the tested concentration range. However, through the extraction of video data, we determined that the tobacco-specific nitrosamine N'-nitrosonornicotine caused a reduction in calcification with similar kinetics as the complete Snus extract. From measurements of actual nitrosamine concentrations in

*Corresponding author: nicolezn@ucr.edu.

**Publisher's Disclaimer:** This is a PDF file of an unedited manuscript that has been accepted for publication. As a service to our customers we are providing this early version of the manuscript. The manuscript will undergo copyediting, typesetting, and review of the resulting proof before it is published in its final citable form. Please note that during the production process errors may be discovered which could affect the content, and all legal disclaimers that apply to the journal pertain.

Author Manuscript Author Manuscript Author Manuscript Author Manuscript

Snus tobacco extract we furthermore conclude that N'-nitrosonornicotine has the potential to be a major trigger of developmental osteotoxicity caused by Snus tobacco.

**Keywords**

Embryonic stem cells; calcification; osteogenesis; developmental toxicity; tobacco; Snus; tobacco-specific nitrosamine; nicotine; N'-nitrosonornicotine

## Introduction

Aside from its well-known detrimental effects that include increased cancer risk, heart disease and chronic obstructive pulmonary disease, tobacco use has been associated with increased risk of osteoporosis and fractures as well as delayed mineralization yield and kinetics during bone healing [1–8]. In dental clinics, smoking is among the most common risk factors for post-tooth-extraction complications [9]. Experiments in mice proved that smoke exposure negatively changed the material properties of bone such that it is more prone to accumulate permanent damage [3]. Indeed, a large cohort study including 14,060 U.S. subjects concluded that smoking and bone mineral density were inversely correlated [10].

Exposure to tobacco smoke has long been known to increase the mother's risk for spontaneous abortions and for premature delivery. In the 1980's it was concluded that cigarette smoke also caused many abnormalities to embryos [11]. Further, some laboratory studies have begun to verify the detrimental effects of tobacco exposure to the embryonic skeleton [12]. Isolated epidemiological human studies have associated smoking while pregnant with lower neonatal bone mass [1] and prepubertal bone mass at age 8 [13–14], although no increased fracture occurrence was reported in children of smoking mothers [15–17]. However, more recent studies find a significant correlation between *in utero* tobacco exposure and childhood fracture risk [2] as well as neonate bone mineral quality [1].

Despite warnings, 10–12% of women in the U.S. consume tobacco products during pregnancy [18], often using so-called 'harm-reduction' tobacco products, which are perceived as safer. Smokeless tobacco, including Snus, falls in this category since it does not yield combustion products when used. Similar to chewing tobacco, consumption of Snus occurs orally: a small tobacco filled pouch is placed between the upper lip and gums and the resulting juice is swallowed. In Nordic European countries, where Snus has been traditionally consumed since the early 19th century, the prevalence of Snus use has increased in recent years as consumption of conventional cigarettes has fallen [19–20]. North America has introduced Snus only in 2006, but market sales have already doubled between 2009 and 2010, with Snus brands establishing themselves among the top 10 moist snuff brands sold in the U.S. just two years after their introduction [21]. Its colorful packaging and sweet flavoring especially markets Snus to youth, young adolescents, and women. Indeed, the use of smokeless tobacco has increased among women of childbearing age both in Sweden and globally [22]. Although Snus is marketed with claims of reduced cancer risk, little is known about its potential harmful effects on developing bone cells.

Author Manuscript Author Manuscript Author Manuscript Author Manuscript

To evaluate the risk of Snus exposure on the human skeleton, in this study, we turn to human embryonic stem cells (ESCs). The differentiation of ESCs mimics the development of an embryo *in vitro* and has been exploited for analysis of risk associated with xenobiotic exposure in many tissues, including bone [23–25]. The genesis of bone from ESCs or within the skeleton ends with the formation of hydroxyapatite from calcium and phosphate. This process of calcification is facilitated by the osteoblast, which secretes a collagenous matrix as the frame work for the hydroxyapatite formation as well as all other extracellular matrix (ECM) proteins necessary for bone function [26]. Among these, osteocalcin (OCN) is uniquely found only in bone tissue, which is why its presence is often used as a biomarker for osteogenesis [27–32]. The ability of osteoblasts to calcify the ECM can also be confirmed by calcium specific stains, such as von Kossa or Alizarin Red [28, 30, 32–34], but this type of assessment is often qualitative.

Quantitatively, absorbent calcium sensitive dyes, such as Arsenazo III, can detect matrix-bound calcium [35]. Because quantification with calcium-sensitive dyes typically requires sacrificing the culture, our lab has used the physical black appearance of the calcified matrix in still bright-field images to quantify the amount of calcium deposited by ESCs as they differentiate and when exposed to xenobiotics [23–25, 36]. The kinetic analysis of this signature dark appearance of the calcified matrix as described in this paper is the cornerstone in the assessment of Snus exposure on such developing cells. With it, we were able to determine the adverse effects of Snus on differentiating osteoblasts, measurable already after 10 days in culture. Furthermore, we were able to pinpoint the tobacco constituent N'-nitrosonornicotine as a potential driving force for the inhibitory outcome of Snus exposure on osteogenesis.

## Materials and Methods

### Cell culture

H9 human embryonic stem cells (hESCs) were obtained from WiCell and were cultured on Matrigel (BD Biosciences) treated culture plates in mTeSR 1 medium (Stem Cell Technologies) as feeder-free cultures at 37°C with 5% $CO_2$ as described [32]. Colonies were passaged every 5 days using accutase treatment (2–4 min at room temperature) and a cell scraper to dislodge cell clumps from the plastic. Cells were used within passages 3–10 after thawing to prevent accumulation of karyotypic abnormalities and screened once a month for mycoplasma contamination.

Human foreskin fibroblasts were provided by Dr. Derrick Rancourt (University of Calgary, Canada) and cultured in high glucose L-glutamine Dulbecco's modified Eagle's medium (DMEM, Corning) with 10% fetal bovine serum (FBS, Atlanta), 1% non-essential amino acids (NEAA, Gibco), and 0.5% penicillin/streptomycin (10,000 units/10,000 units, Gibco).

### Osteogenic differentiation of embryonic stem cells

Differentiation was induced from confluent hESCs by the addition of control differentiation medium (CDM) composed of DMEM containing 15% FBS (Atlanta Biologicals), 1% (v/v) non-essential amino acids, 50 U/ml penicillin, 50 μg/ml streptomycin, and 0.1 mM β-

Author Manuscript Author Manuscript Author Manuscript Author Manuscript

mercaptoethanol [32]. Osteogenic differentiation medium composed of CDM supplemented with $1.2\times10^{-7}$ M 1,25α(OH)$_2$ Vitamin D$_3$ (VD3; Calbiochem), 0.1 mM β-glycerophosphate (βGP), and 20.8 μg/ml ascorbic acid (AA) was used from day 5 of differentiation onward [28, 30, 32]. Non-osteogenic cultures were continuously cultured in CDM.

### Immunocytochemistry

Cells were rinsed with phosphate buffered saline (PBS) and fixed in 4% paraformaldehyde at 4°C for 1 hour. Fixed cells were permeabilized with 0.1% Triton X-100/PBS and stained with anti-OCN (AbCam; AB1857) in 4% FBS/PBS overnight at 4°C. A secondary anti-rabbit IgG conjugated to Alexa Fluor 546 (Invitrogen; A10040) in 10% FBS/PBS was incubated for 2 hours at room temperature. Cultures were counterstained with 4',6-diamidino-2-phenylindole (DAPI) and visualized using a Nikon Eclipse Ti microscope.

### Cytochemical staining

Fixed cells were stained with 2% (w/v) Alizarin Red solution for 5 min and then washed with PBS followed by increasing concentrations of ethanol (70%, 80%, 90%, 100%). For von Kossa stain, cultures were stained with 5% silver nitrate solution under a strong light source for one hour. Cultures were washed three times with water and fixed with 5% sodium thiosulfate for 2 min.

### Detection of calcium

To quantify calcium content, cells were lysed with radio-immunoprecipitation assay (RIPA) buffer (1% NP40, 0.5% sodium deoxycholate, 0.1% sodium dodecyl sulfate, in PBS). The cell lysate was assayed with Arsenazo III (Genzyme) and the change in absorbance measured at 655 nm in an iMark microplate reader (BioRad). Absorbances were compared to a $CaCl_2$ calcium standard and total calcium content normalized to the total protein content determined by a Lowry assay as described [35]. Each biological replicate was tested in 5 technical replicates.

### Image acquisition and analysis

Differentiating cultures were placed inside the Nikon Biostation CT, a hybrid and automated incubator that contains a phase contrast microscope and maintains the culture at 37°C with 5% $CO_2$. Phase contrast images were taken every 12h for a period of 20 days from 10 separate areas within the culture plate. Images were assembled to create time-lapse videos (Fig. 1). Time lapse videos were analyzed using the Matrix Laboratory (MatLab) program, designed to automatically segment black calcified areas from the individual phase contrast images from the time-lapse video using a manual threshold for pixels with an intensity value of 33 or less as described [37]. Pixels corresponding to grey areas, which arise from three-dimensional cell growth, were removed to create segmented images of black-appearing calcified regions only. Remaining segmented pixels were counted to quantitatively represent the degree of calcification from each image.

Concentration response curves for tobacco toxicants were obtained by normalizing the calcium pixel counts in images of each concentration from a treated sample with the calcified pixel counts from an untreated sample represented as percentage. To determine the

Author Manuscript Author Manuscript Author Manuscript Author Manuscript

calcification rate the amount of calcified pixels from each image at a designated time point were subtracted from the amount of calcified pixels at t0 and divided by the hours of elapsed time.

### Exposure with tobacco extract and constituents

Tobacco extract was made by incubating 10 g of Camel or Marlboro Snus in 100 ml of DMEM with 15% FBS overnight. The extract was centrifuged at 450×g for 10 min at room temperature and the supernatant again centrifuged at 13,000×g for 1 hour to remove finer tobacco debris. The pH was adjusted to 7.4 and the extract filter sterilized. Nicotine, N'-Nitrosoanabasine (NAB), (R,S)-N-nitroso anatabine (NAT), 4-(methylnitrosamino)-1-(3-pyridyl)-1-butanone (NNK) and N'-nitrosonornicotine (NNN), (Toronto Research Chemicals), components previously identified in tobacco [38, 39], were diluted in DMEM to yield a stock solution of 48 mM. Cell treatment started with d0 of differentiation and continued throughout. Medium including chemicals freshly diluted to final concentrations was changed every other day.

### MTT assay

Osteoblast health in response to tobacco extract and constituent exposure was determined by 3-[4,5-dimethylthiazol-2-yl]-2,5-diphenylterazolium bromide (MTT) assay. Briefly, cells were incubated with MTT (120 mg/ml) at 37°C for 3 h. After the supernatant was removed, 0.04 mol/l HCl in isopropanol was added to each well, and the optical density of the solution was read at 595 nm in an iMark™ microplate reader (Bio-Rad) [23–25].

### Determination of nicotine and tobacco-specific nitrosamine content

Concentrations of nicotine and tobacco specific nitrosamines in Camel Snus tobacco extract were measured commercially by Enthalpy Analytical (Henrico, VA).

### Statistics

All experiments were run in biological triplicate. Arsenazo III-reagent based calcium assays were run in biological quintuplicate and video bioinformatic assessment was performed from a total of 30 areas within three independent culture wells. Values represent means ± s.d. Statistical assessment was performed with a t-test when appropriate (http://www.graphpad.com/quickcalcs/ttest1/) or One-Way ANOVA with Holm-Sidak posthoc test when multiple groups were compared (SigmaPlot). A *P*-value below 0.05 was considered significant. Half-maximal inhibitory doses of cytotoxicity and differentiation (IC50) were taken from concentration-response curves and embryotoxicity classes calculated according to [40–41].

## Results

### Snus tobacco extracts are inhibitory to osteogenic differentiation

In culture, calcification from emerging hESC-derived osteoblasts possesses a distinct appearance when viewed under phase-contrast microscopy (Fig. 2A) as was previously found for mouse, rhesus, and marmoset ESCs [28, 42–43]. This signature appearance is

Author Manuscript Author Manuscript Author Manuscript Author Manuscript

viewed as dense black clusters that result from the inability of light to pass through calcified matrix. These areas are immuno-positive for OCN, a bone-specific protein found in the bone matrix, and are composed of calcium as determined by Alizarin Red S (Fig. 2A) [28, 32, 42–43]. These dense black areas could be removed with the calcium chelator EDTA (Fig. 2B), are not present when osteogenic factors were withheld from the media (denoted as non-osteogenic) (Fig. 2C, D), and their increased levels correlate with an up-regulation in osteoblast-specific gene expression patterns [32].

We next exploited this calcification of the extracellular matrix, as a unique measure of osteoblast function, to determine the potential developmental toxicity of two types of Snus tobacco extract (STE), from the Marlboro and the Camel brand and contrasted it to the cytotoxicity, assessed with MTT assay [23–25]. (Fig. 2D). For both extracts, calcification was significantly inhibited in a concentration-dependent manner when hESCs were tested. Specifically, in a concentration range between 0.1–3% STE, the extracts decreased calcification independently of cytotoxicity. In the highest concentrations tested, the extracts were both cytotoxic and inhibitory to differentiation. Human fibroblasts, who represent fully differentiated somatic cells in this assay, were even more sensitive to the extracts and began to die at lower concentrations. When applying a biostatistical model that contrasts the IC50 values of all endpoints [40–41] (Fig. 2E), both Snus extracts classified as strongly embryotoxic, which predicts them to be detrimental to developing skeletal cells.

## Identification of an early detection time point based on calcification kinetics

While this assay was seemingly predictive of the developmental adverse effects of Snus, a major disadvantage of it is its long duration. To determine whether assessment could be made earlier than at day 20, we hypothesized that the black appearance of the calcified matrix in phase contrast images could be exploited to measure hESC differentiation yield in a kinetic manner, which would allow us to determine a time point in which calcification rose measurably over the background. To do so, live cultures of osteogenically induced and non-osteogenically induced hESCs were imaged as time-lapse videos using the Nikon Biostation CT to follow their commitment into the osteogenic lineage. Images from all time points in the sequence were then extracted from the video and black-appearing calcified areas were segmented [37] from all images (Fig. 3A). The first day that calcification was significantly increased over non-osteogenically induced cultures, as judged from multiple different sets of experiments, was identified to be day 10 (Fig. 3B, C).

To assess differentiation kinetics even further, we next determined the calcification rate of the cultures from the time-lapse video [37], which represents the added amount of calcification between to selected time points. Based on this calcification rate, we could determine that the amount of calcification added to the ECM of the H9 cells accelerated as time progressed (Fig. 3D, E).

## Snus tobacco extract adversely affects hESC calcification yield and kinetics

We next aimed to measure calcification from time-lapse videos to study the embryotoxicity of Camel Snus tobacco extract, the more toxic of the two Snus tobacco products tested, in more detail. Photomicrographs derived from key time-points of time-lapse videos created

Author Manuscript Author Manuscript Author Manuscript Author Manuscript

from osteogenically differentiating hESCs treated with STE morphologically revealed no overt calcium deposition at 1% STE (Fig. 4A) or higher (Fig. 2D).

The image-based calcification assay was then used to quantify calcium deposition in concentrations below 1%. The lowest dose tested (0.001% STE) did not cause any significant changes in the number of segmented pixels compared to the solvent control cultures (Fig. 4B). However, at doses higher than that, a concentration-dependent decrease in calcification was noted that was first significant at d8 of culture. Typically, toxicity assays will normalize the effect in any given endpoint to the solvent control [23–25, 40–41]. Normalizing the calcification output of a tobacco treated sample to the solvent control, the image-based program detected differences between various tobacco concentrations again supporting the notion that higher doses of STE decreased calcification (Fig. 4C). In addition, both analyses suggested an early delay in calcification (d5–10) coupled with a dose-dependent overall yield at the maturation stage (d20). In line with these findings, the calcification rates showed significantly slower calcification profiles dependent on STE concentration (Fig. 4D).

We then exploited this image-based kinetic information on calcification to set a time point for earlier screening than d20, which is currently the norm [23–25, 44]. To do this, we decided on day 10, since it produced the first stable and significant difference beyond a baseline threshold (compare Fig. 3B, C). Based on such a d10 analysis, a concentration response curve was generated (Fig. 4E) and a half-maximal inhibition of differentiation ($ID_{50}$) determined to be 0.12 ± 0.09% STE. A concentration-response curve generated from d20 data obtained with the traditional dye-based calcification assay revealed a similar $ID_{50}$ value of 0.12 ± 0.05% (Fig. 4F).

## Nicotine is not a major contributor to the osteotoxic effect of Snus tobacco extract

Tobacco is a complex mixture of at least 5000 chemicals that are toxic and carcinogenic and it is still undetermined which of these chemicals lead to the observed changes as presented above. The most recognized component found in tobacco smoke is nicotine, which is responsible for the addictive properties associated with cigarette use [45–46]. Its less recognized effects include the lowering of 25-hydroxyvitamin D serum levels as was described for adult female rats suggesting that nicotine may cause issues with body storage of vitamin D, a hormone necessary for bone turnover [47]. Likewise, nicotine caused a reduction in bone mineral content [47] In the adult, nicotine can complicate bone healing and may significantly decrease bone mineral content [48]. In addition, epidemiological studies showed that post-menopausal women who smoke lose more cortical bone than non-smokers [49], suggesting a link between tobacco and osteoporosis. Thus, as nicotine has been proposed to influence bone formation previously, we used our image-based calcification assay to determine whether nicotine was the component in tobacco responsible for the observed decrease in calcification.

The results showed no discernible difference in culture morphology in any of the concentrations of nicotine tested (Fig. 5A). Segmenting the pixels associated with calcification revealed a seeming increase in calcification in all tested concentrations, however these were not statistically significant (Fig. 5B, C). Calculations for the

Author Manuscript Author Manuscript Author Manuscript Author Manuscript

calcification rate confirmed the nicotine treated samples exhibited the same calcification kinetics as the untreated sample (Fig. 5D). Concentration-response curves based on both image analysis and Arsenazo III-reagent calcium measurement did not show any significant reduction in calcification yield (Fig. 5E, F). In conclusion, this data implies that the change in the functional output of osteoblasts derived from hESCs observed after exposure to whole tobacco smoke extract was not due to the nicotine component.

### N'-nitrosonornicotine potentially contributes to the toxic effect of Snus tobacco extract

Tobacco specific nitrosamines (TSNAs) are another set of major components in tobacco [50]. They are widely accepted to contribute to its cancer risk [51–52], but their effect on the osteogenic lineage is less well understood. To determine whether TSNAs had a contributory effect to the observed developmental osteotoxicity of STE, we next treated differentiating hESCs with various concentrations of N'-Nitrosoanabasine (NAB), (R,S)-N-nitroso anatabine (NAT), 4-(methylnitro-samino)-1-(3-pyridyl)-1-butanone (NNK) and N'-nitrosonornicotine (NNN), and measured the outcome of exposure with regard to cytotoxicity and osteogenic differentiation yield. Human foreskin fibroblasts were also exposed to determine the effects of the chemicals on fully differentiated cells. The corresponding data suggested that neither NAT nor NNK caused any adverse effects in the tested range. In contrast, NAB similarly reduced calcification and cellular viability of the differentiating osteoblasts with similar half-maximal inhibitory doses (Fig. 6A, B).

However, the cytotoxic effect of NAB did not seem to be specific to developing osteoblasts only, since the fibroblasts were equally sensitive. In contrast, NNN decreased calcification output at concentrations below such that caused cytotoxicity in either cell line, suggesting a specific effect on osteoblast cell fate. The decrease in calcification occurred over a large concentration range, with statistically significant decreases that were lower than the solvent control starting at 85 pg/ml of NNN. Thereby, only NNN exhibited an inhibitory effect on osteoblast differentiation at concentrations actually present in the STE extract (Fig. 6A, B).

Next, we used image analysis on NNN exposed hESCs to determine the developmental toxicity of NNN in more detail. Visual inspection of the segmentation of calcified areas in images of NNN treated cells suggested that NNN had a concentration-dependent effect on calcification as already determined with the Arsenazo III reagent-based calcium assay (Fig. 7A). This finding was also confirmed with the quantitative pixel count analysis (Fig. 7B, C). However, the determination of the calcification rate discovered a novel parameter of the defect, which was that low concentrations of NNN were associated with late mineralization defects, while higher concentrations exhibited early differentiation inhibition (Fig. 7D).

Comparison of the image-based calcification assay on d10 (Fig. 7E) with the Arsenazo III reagent-based method as assayed on d20 (Fig. 7F) confirmed the dose-dependent decline in calcification as a result of NNN treatment with the image-based analysis being slightly more sensitive as the conventional assay. The half-maximal inhibitory dose that was determined for with the image analysis was 0.115 μg/ml, which was very close to the level of 0.0618 μg/ml that was found in the STE extract.

Author Manuscript Author Manuscript Author Manuscript Author Manuscript

## Discussion

In this study, we have successfully used image analysis and quantification of data performed from a series of time-lapsed images in the form of videos to quantify calcification of osteoblasts derived from human ESCs and to characterize the differences in calcification in response to a major environmental toxicant. The time-lapsed image-based calcification assay that was used in this study analyzes the complete calcification process, d0 to d20, from one live culture. The kinetic manner in which it was used facilitated a reduction in assay time when screening the effects of tobacco extracts and its constituents on osteogenesis due to the identification of the earliest time point at which significant differences could be detected between the treated solvent control and a tested concentration of chemical. In addition, the calcification rate determined that calcification was slightly delayed upon exposure to Snus tobacco extract.

There are four cellular mechanism for the induction of skeletal defects during embryogenesis: environmental toxicants may a) change the activity of metabolic enzymes, b) induce permanent epigenetic changes [53], c) reduce cell numbers [54–56] or 4) alter the identity of progenitor cells [57]. Evidence from human studies so far suggest that skeletal development might be programmed as a consequence of the first three of these mechanisms. However, the fact that calcification reached a limit early on during the differentiation process and failed to further increase over time as seen with the video bioinformatic approach may provide first evidence that the fourth mechanism is also at play, as it points to a defect in differentiation early on in development.

Indeed, cigarette smoking has been suggested to have adverse effects on bone tissue. For example, smoking increased the occurrence of developing osteopathies, such as osteoporosis [58–60] and Legg-Calve-Perthes Disease [61] and has been implicated in delayed healing of fractured bones [62–63]. Based on the results presented here, negative effects of tobacco on the adult bone are not surprising, given that osteogenesis is a life-long process. Bone matrix is constantly digested by the osteoclasts only to be renewed by the osteoblasts, in a process called bone remodeling. During bone remodeling, osteoblasts arise from the differentiation of mesenchymal cells that reside in the bone marrow, which under influence of tobacco may not secrete adequate amounts of bone matrix or undergo apoptosis prematurely.

Our results also corroborate newer data that is suggesting detrimental effects of prenatal tobacco exposure on the embryonic and newborn skeleton. Among other environmental factors it accounts for the high frequencies of many congenital anomalies in infants [64], including such that affect the skeleton. Limited research in young adults and immature animals suggests a detrimental effect of tobacco on bone during growth [65] and more recent studies correlate in utero exposure to lowered neonate bone mineral quality [1], consequently leading to increased childhood fracture risk [2]. We add here to the growing body of evidence the designation of Snus tobacco extract as a potential developmental toxicant, specifically in the osteogenic lineage.

Our further studies suggested that nicotine was not the primary culprit causing this adverse effect. In the light of some prior studies our results are surprising. In the adult, for instance,

Author Manuscript Author Manuscript Author Manuscript Author Manuscript

nicotine consumption from tobacco use and cigarette smoking can lead to complications in bone remodeling and healing, as determined from a reduction in bone mineral content (BMC). In a cohort study to determine the effects of cigarette smoking on bone mass, Gerdhem and Obrant found a significant decrease in BMC in the femoral neck, tibia, calcaneus, as well as in the lumbar spine and bones in the hand [48]. Also, in rat calvarial osteogenic cells and clonal mouse calvarial preosteoblastic MC3T3-E1 cells, nicotine caused a reduction in ECM calcium content [66]. However, the mentioned studies found the inhibitory effect of nicotine at relatively high concentrations of 250 μg/ml. In arterial blood, this concentration is not reached after smoking a cigarette [67]. Concentrations can reach up to 0.1 μg/ml, but average between 0.02–0.06 μg/ml [67–70]. While nicotine crosses the placental barrier and is thought to accumulate in fetal serum and amniotic fluid in slightly higher concentrations than in maternal serum [71], the *in vitro* concentrations that cause osteoblast toxicity are not reached *in vivo*. In contrast, our study tested nicotine in these physiological ranges and did not detect any adverse effects.

In line with our findings, other prior literature has also doubted that the reproductive toxicity of cigarette smoking is primarily related to nicotine [71]. Instead, they conclude that the cumulative abnormalities produced by the various toxins in cigarette smoke are probably responsible for the numerous adverse reproductive outcomes associated with smoking. Indeed, even with a sufficiently high intake of nicotine [72], its effects on bone biomechanical properties are marginal [73–76], while the complete chemical mixture found in tobacco smoke jeopardized bone integrity at an implant interface [77].

Instead, we show here that during developmental bone toxicity, a major culprit might be the TSNAs, specifically NNN. While the use of chewing tobacco reduces exposure to chemicals that are produced during combustion, Snus still contains a high amount of TSNAs [78]. TSNAs are classified as carcinogens but have also been shown to cause adverse health effects in mammalian cells due to non-cancerogenic mechanisms, such as promotion of oxidative stress and inflammation [79–80]. In fact, efforts are under way to limit TSNA content in Snus and tobacco companies are already marketing low TSNA Snus [78]. Designated as such a low TSNA Snus, the extract of the Camel Original Snus tested here still contained a level of TSNAs, specifically NNN, that was near the half-maximal inhibitory dose found for this chemical. Moreover, NNN was found to have detrimental effects to osteoblast differentiation at 85 pg/ml, a concentration much lower than the determined half-maximal inhibitory dose and more importantly within proximity to the range of 8.9–47.2 pg/ml NNN measured in urine of tobacco consumers [81–82]. Hence, there is reason for concern that Snus consumption may be detrimental to differentiating osteoblasts also in the developing embryo and that NNN may be a major contributor to the detrimental effect of Snus on differentiating osteoblasts.

We conclude this because NNN exposure not only reduced overall calcification yield, as did Snus exposure, but also because the kinetics with which calcification was affected were very similar. We were able to deduce the differentiation kinetics due to the time-dependent assessment of calcification from video-derived images. Ultimately, this method can be used to generate calcification curves and identify $ID_{50}$ of other constituents of Snus with a simple variation in the protocol.

Author Manuscript Author Manuscript Author Manuscript Author Manuscript

## Acknowledgements

Experiments in this study were supported by a New Investigator Award and a High Impact Pilot Award from the Tobacco Related Disease Research Program (TRDRP) [grant numbers 19KT-0017 and 25IP-0018] and a grant from the Center for Alternatives to Animal Testing [grant number 2013–11], respectively. IKCM is a TRDRP Dissertation Awardee [20DT-0038] and National Science Foundation IGERT fellow of Video Bioinformatics [NSF grant 903667]. NRLS acknowledges the support from a TRDRP Cornelius Hopper Diversity Award and a fellowship from the International Foundation for Ethical Research. BB acknowledges the support from NSF IGERT on Video Bioinformatics [NSF grant 903667]. JVM is a California Institute for Regenerative Medicine (CIRM) Bridges fellow. NzN is funded by an RO1 (DE025330) from the National Institutes of Dental and Craniofacial Research. The authors would like to thank the Stem Cell Core Facility of the University of California Riverside, a CIRM funded shared facility, for providing access to the Biostation CT.

## References

1. Godfrey K, Walker-Bone K, Robinson S, Taylor P, Shore S, Wheeler T, Cooper C. Neonatal bone mass: influence of parental birthweight, maternal smoking, body composition, and activity during pregnancy. J Bone Miner Res 2001;16:1694–03. [PubMed: 11547840]
2. Parviainen R, Auvinen J, Pokka T, Serlo W, Sinikumpu JJ. Maternal smoking during pregnancy is associated with childhood bone fractures in offspring – A birth-cohort study of 6718 children. Bone 2017;101:202–5. [PubMed: 28479497]
3. Seeman E, Melton EJ, O'Fallon WM, et al. Risk factors for spinal osteoporosis in men Am J Med, 75 (1983), pp. 977–983 [PubMed: 6650552]
4. Daniell HW. Osteoporosis of the slender smoker Arch Intern Med, 136 (1976), pp. 298–304 [PubMed: 946588]
5. Cooper C, Barker DJ, Wickham C. Physical activity, muscle strength, and calcium intake in fracture of the proximal femur in Britain BMJ, 297 (1988), pp. 1443–1446 [PubMed: 3147008]
6. Blum M, Harris SS, Must A, Phillips SM, Rand WM, Dawson-Hughes B. Household tobacco smoke exposure is negatively associated with premenopausal bone mass. Osteoporos Int 2002;13:663–8. [PubMed: 12181626]
7. Izumotani K, Hagiwara S, Izumotani T, Miki T, Moril H, Nishizawa A (2003) Risk factors for osteoporosis in men. J Bone Miner Metab 2003;21:86–90. [PubMed: 12601572]
8. Ortego-Centeno N, Munoa-Torres M, Jodar E, Hernandez Quero J, Jurado-Duce A, de la Higuera Torris-Puchol J Effect of tobacco consumption on bone mineral density in healthy young males. Calcif Tissue Int 1997;60:496–500. [PubMed: 9164822]
9. Ozkan A, Bayar GR, Altug HA, Sencimen M, Dogan N, Gunaydin Y, Ergodan E. The effect of cigarette smoking on the healing of extraction sockets: an immunohistochemical study. J Craniofac Surg 2014;25(4):e397–402. [PubMed: 24481166]
10. Benson BW, Shulman JD. Inclusion of tobacco exposure as a predictive factor for decreased bone mineral content. Nicotine Tob Res 2005;7(5):719–24. [PubMed: 16191742]
11. Ejaz S, Ashraf M, Nawaz M, Lim CW, Kim B. Anti-angiogenic and teratological activities associated with exposure to total particulate matter from commercial cigarettes. Food and Chemical Toxicology 2009;47:368–76. [PubMed: 19084571]
12. Paulson R, Shanfeld J, Sachs L, Ismail M, Paulson J. Effect of smokeless tobacco on the development of the CD-1 mouse fetus. Teratog Carcinog Mutagen 1988;8(2):81–93. [PubMed: 2899919]
13. Jones G, Riley M, Dwyer T. Maternal smoking during pregnancy, growth and bone mass in prepubertal children. J Bone Miner Res 1999;14:147–52.
14. Micklesfield L, Levitt N, Dhansay M, Norris S, van der Merwe L, Lambert E. Maternal and early life influences on calcaneal ultrasound parameters and metacarpal morphometry in 7-to 9-year-old children. J Bone Miner Metab 2006;24:235–42. [PubMed: 16622737]
15. Jones IE, Williams SM, Goulding A. Associations of birth weight and length, childhood size, and smoking with bone fractures during growth: evidence from a birth cohort study. Am J Epidemiol 2004;159:343–50. [PubMed: 14769637]

Author Manuscript Author Manuscript Author Manuscript Author Manuscript

16. Jones G, Hynes KL, Dwyer T. The association between breastfeeding, maternal smoking in utero, and birth weight with bone mass and fractures in adolescents: a 16-year longitudinal study. Osteoporos Int 2013;24(5):1605–11. [PubMed: 23149649]
17. Hallal PC, Siqueira FV, Menezes AM, Araújo CL, Norris SA, Victora CG. The role of early life variables on the risk of fractures from birth to early adolescence: a prospective birth cohort study. Osteoporos Int 2009;20(11):1873–9. [PubMed: 19271096]
18. Tong VT, Jones JR, Dietz PM, D'Angelo D, Bombard JM, CDC. Trends in smoking before, during, and after pregnancy - Pregnancy Risk Assessment Monitoring System (PRAMS), United States, 31 sites, 2000–2005. MMWR Surceill Summ 2009;58(4):1–29.
19. Pedersen W, von Soest T. Tobacco use among Norwegian adolescents: from cigarettes to snus. Addiction 2014;109(7):1154–62. [PubMed: 24521070]
20. Lund M, Lund KE, Halkjelsvik T. Contrasting smokers' and snus users' perceptions of personal tobacco behavior in norway. Nicotine Tob Res 2014;16(12):1577–85 [PubMed: 24991039]
21. Delnevo CD, Wackowski OA, Giovenco DP, Manderski MT, Hrywna M, Ling PM. Examining market trends in the United States smokeless tobacco use: 2005–2011. Tob Control 2014;23:107–12. [PubMed: 23117999]
22. Connolly GN, Alpert HR. Trends in the use of cigarettes and other tobacco products, 2000– 2007. JAMA 2008;299:2629–30. [PubMed: 18544722]
23. zur Nieden NI, Davis LA, Rancourt DE. Comparing three novel endpoints for developmental osteotoxicity in the embryonic stem cell test. Toxicol Appl Pharmacol 2010;247(2):91–97. [PubMed: 20576515]
24. zur Nieden NI, Baumgartner L. Assessing developmental osteotoxicity of chlorides in the embryonic stem cell test. Reprod Toxicol 2010;30(2):277–83. [PubMed: 20447454]
25. Walker L, Baumgartner L, Ast J, Keller KC, Trettner S, zur Nieden NI. Non-human primate and rodent embryonic stem cells are differentially sensitive to teratogens. Tox. Reports 2014;2:165–74.
26. Boskey AL. Matrix proteins and mineralization: an overview. Connect Tissue Res 1996;35(1–4): 357–63. [PubMed: 9084675]
27. Buttery LD, Bourne S, Xynos JD, Wood H, Hughes FJ, Hughes SP, Episkopou V, Polak JM. Differentiation of osteoblasts and in vitro bone formation from murine embryonic stem cells. Tissue Eng 2001;7(1):89–99. [PubMed: 11224927]
28. zur Nieden NI, Kempka G, Ahr HJ. In vitro differentiation of embryonic stem cells into mineralized osteoblasts. Differentiation 2003;71(1):18–27. [PubMed: 12558600]
29. Sottile V, Thomson A, McWhir J. In vitro osteogenic differentiation of human ES cells. Cloning Stem Cells 2003;5(2):149–55. [PubMed: 12930627]
30. Ding H, Keller KC, Martinez IK, Geransar RM, zur Nieden KO, Nishikawa SG, Rancourt DE, zur Nieden NI. NO-β-catenin crosstalk modulates primitive streak formation prior to embryonic stem cell osteogenic differentiation. J Cell Sci 2012;125(Pt 22):5564–77. [PubMed: 22946055]
31. Rutledge KE, Cheng Q, Pryzhkova M, Harris G, Jabbarzadeh E. Enhanced differentiation of human embryonic stem cells on ECM-containing osteomimetic scaffolds for bone tissue engineering. Tissue Eng Part C Methods 2014;20(11):865–74. [PubMed: 24634988]
32. Sparks NRL, Martinez IKC, Soto CH, zur Nieden NI. Low osteogenic yield in human pluripotent stem cell lines correlates with differential methylation of neural crest associated promoters. Stem Cells 2018;36(3):349–62. [PubMed: 29193426]
33. Puchtler H, Meloan SN, and Terry MS. On the history and mechanism of alizarin and alizarin red S stains for calcium. J Histochem Cytochem 1969;17(2):110–24. [PubMed: 4179464]
34. Rungby J The von Kossa reaction for calcium deposits: silver lactate staining increases sensitivity and reduces background. Histochem J 1993;25(6):446–51. [PubMed: 8360080]
35. Davis LA, Dienelt A, and zur Nieden NI. Absorption-based assays for the analysis of osteogenic and chondrogenic yield. Methods Mol Biol 2011;690:255–72. [PubMed: 21042998]
36. zur Nieden NI, Price FD, Davis LA, Everitt RE, Rancourt DE. Gene profiling on mixed embryonic stem cell populations reveals a biphasic role for beta-catenin in osteogenic differentiation. Mol Endocrinol 2007;21(3):674–85. [PubMed: 17170073]
37. Martinez IKC, Bhanu B, zur Nieden NI. Video-based calcification assay: A novel method for kinetic analysis of osteogenesis in live cultures. MethodsX 2018; co-submitted with this revision

Author Manuscript Author Manuscript Author Manuscript Author Manuscript


38. Benowitz NL, Hukkanen J, Jacob P 3rd. Nicotine chemistry, metabolism, kinetics and biomarkers. Handb Exp Pharmacol 2009;(192):29–60. [PubMed: 19184645]
39. Hecht SS, Ornaf RM, Hoffmann D. Chemical studies on tobacco smoke. XXXIII. N' nitrosonornicotine in tobacco: analysis of possible contributing factors and biologic implications. J Natl Cancer Inst 1975;54(5):1237–44. [PubMed: 236398]
40. Genschow E, Spielmann H, Scholz G, Seiler A, Brown N, Piersma A, Brady M, Clemann N, Huuskonen H, Paillard F, Bremer S, Becker K. The ECVAM international validation study on in vitro embryotoxicity tests: results of the definitive phase and evaluation of prediction models. European Centre for the Validation of Alternative Methods. Altern Lab Anim 2002;30(2):151–76.
41. Genschow E, Scholz G, Brown N, Piersma A, Brady M, Clemann N, Huuskonen H, Paillard F, Bremer S, Becker K, Spielmann H. Development of prediction models for three in vitro embryotoxicity tests in an ECVAM validation study. In Vitr Mol Toxicol 2000;13(1):51–66. [PubMed: 10900407]
42. Dienelt A, zur Nieden NI. Hyperglycemia impairs skeletogenesis from embryonic stem cells by affecting osteoblast and osteoclast differentiation. Stem Cells Dev 2011;20(3):465–74. [PubMed: 20939707]
43. Trettner S, Findeisen A, Taube S, Horn P, Sasaki E, zur Nieden NI. Osteogenic induction from primate embryonic stem cells cultured in feeder-dependent and feeder-independent conditions. Osteoporosis Int 2014;25(4):1255–66.
44. Kuske B, Pulyanina PY, zur Nieden NI. Embryonic stem cell test: stem cell use in predicting developmental cardiotoxicity and osteotoxicity. Methods Mol Biol 2012;889:147–79. [PubMed: 22669664]
45. Rickert WS, Robinson JC, Collishaw N. Yields of tar, nicotine, and carbon monoxide in the sidestream smoke from 15 brands of Canadian cigarettes. Am J Public Health 1984;74(3):228–31. [PubMed: 6696152]
46. Talhout R, Schulz T, Florek E, van Benthem J, Wester P, Opperhuizen A. Hazardous compounds in tobacco smoke. Int. J. Environ. Res. Public. Health 2011;8(2):613–28. [PubMed: 21556207]
47. Fung YK, Iwaniec UT, Cullen DM, Akhter MP, Haven MC, Timmins P (1999) Long-term effects of nicotine on bone and calcitropic hormones in adult female rats. Pharmacol Toxicol 85:181–187 [PubMed: 10563517]
48. Gerdhem P, Obrant KJ. Effects of cigarette-smoking on bone mass as assessed by dual-energy X-ray absorptiometry and ultrasound. Osteoporos Int 2002;13(12):932–6. [PubMed: 12459935]
49. Behnke M, Smith VC; Committee on Substance Abuse; Committee on Fetus and Newborn. Prenatal substance abuse: short- and long-term effects on the exposed fetus. Pediatrics 2013;131(3):e1009–24. [PubMed: 23439891]
50. Rühl C, Adams JD, Hoffmann D. Chemical studies on tobacco-specific N-nitrosamines in the smoke of selected cigarettes from the U.S.A., West Germany, and France. J Anal Toxicol 1980;4(5):255–9. [PubMed: 7442138]
51. Hecht SS. It is time to regulate carcinogenic tobacco-specific nitrosamines in cigarette tobacco. Cancer Prev Res (Phila) 2014;7(7):639–47. [PubMed: 24806664]
52. Xue J, Yang S, Seng S. Mechanisms of Cancer Induction by Tobacco-Specific NNK and NNN. Cancers (Basel), 2014;14;6(2):1138–56. [PubMed: 24830349]
53. Brown SA, Rogers LK, Dunn JK. Development of cholesterol homeostatic memory in the rat is influenced by maternal diets. Metabolism 1990;39:468–73. [PubMed: 2336034]
54. McLeod KI, Goldrick RB, Whyte HM. The effect of maternal malnutrition on the progeny in the rat: studies on growth, body composition and organ cellularity in first and second generation progeny. Aust J Exp Biol Med Sci 1972;50:435–46. [PubMed: 4629706]
55. Snoeck A, Remacle C, Reusens B, Hoet JJ. Effect of a low protein diet during pregnancy on the fetal rat endocrine pancreas. Biol Neonate 1990;57:107–18. [PubMed: 2178691]
56. Matsui R, Thurlbeck WM, Fujita Y. Connective tissue, mechanical, and morphometric changes in the lungs of weanling rats fed a low protein diet. Pediatr Pulmonol1989;7:159–66. [PubMed: 2797930]
57. Godfrey KM, Barker DJP, Osmond C. Disproportionate fetal growth and raised IGE concentration in adult life. Clin Exp Allergy 1994;24:641–48. [PubMed: 7953946]

Author Manuscript Author Manuscript Author Manuscript Author Manuscript


58. Ayo-Yusuf OA, Olutola BG. Epidemiological association between osteoporosis and combined smoking and use of snuff among South African women. Niger J Clin Pract 2014;17(2):174–7. [PubMed: 24553027]
59. Iqbal J, Sun L, Cao J, Yuen T, Lu P, Bab I, Leu NA, Srinivasan S, Wagage S, Hunter CA, Nebert DW, Zaidi M, Avadhani NG. Smoke carcinogens cause bone loss through the aryl hydrocarbon receptor and induction of Cyp1 enzymes. Proc Natl Acad Sci U S A 2013;110(27):11115–20. [PubMed: 23776235]
60. Brook JS, Balka EB, Zhang C. The smoking patterns of women in their forties: their relationship to later osteoporosis. Psychol Rep 2012;110(2):351–62. [PubMed: 22662390]
61. Daniel AB, Shah H, Kamath A, Guddettu V, Joseph B. Environmental tobacco and wood smoke increase the risk of Legg-Calvé-Perthes disease. Clin Orthop Relat Res 2012;470(9):2369–75. [PubMed: 22090357]
62. Sloan A, Hussain I, Maqsood M, Eremin O, El-Sheemy M. The effects of smoking on fracture healing. Surgeon 2010;8(2):111–6. [PubMed: 20303894]
63. Moghaddam-Alvandi A, Zimmermann G, Hammer K, Bruckner T, Grützner PA, von Recum J. Cigarette smoking influences the clinical and occupational outcome of patients with tibial shaft fractures. Injury 2013 11;44(11):1670–1. [PubMed: 22935593]
64. Stillerman KP, Mattison DR, Giudice LC, Woodruff TJ. Environmental exposures and adverse pregnancy outcomes: a review of the science. Reprod Sci 2008;15(7):631–50. [PubMed: 18836129]
65. Iwaniec UT, Fung YK, Cullen DM, Akhter MP, Haven MC, Schmid M. Effects of nicotine on bone and calciotropic hormones in growing female rats. Calcif Tissue Int 2000;67(1):68–74. [PubMed: 10908416]
66. Yuhara S, Kasagi S, Inoue A, Otsuka E, Hirose S, Hagiwara H. Effects of nicotine on cultured cells suggest that it can influence the formation and resorption of bone. Eur J Pharmacol 1999;383(3): 387–93. [PubMed: 10594333]
67. Gourlay SG, Benowitz NL. Arteriovenous differences in plasma concentration of nicotine and catecholamines and related cardiovascular effects after smoking, nicotine nasal spray, and intravenous nicotine. Clin Pharmacol Ther 1997;62(4):453–63. [PubMed: 9357397]
68. Henningfield JE, Keenan RM. Nicotine delivery kinetics and abuse liability. J Consult Clin Psychol 1993;61(5):743–50. [PubMed: 8245272]
69. Lunell E, Molander L, Ekberg K, Wahren J. Site of nicotine absorption from a vapour inhaler--comparison with cigarette smoking. Eur J Clin Pharmacol 2000;55(10):737–41. [PubMed: 10663452]
70. Rose JE, Behm FM, Westman EC, Coleman RE. Arterial nicotine kinetics during cigarette smoking and intravenous nicotine administration: implications for addiction. Drug Alcohol Depend 1999;56(2):99–107. [PubMed: 10482401]
71. Dempsey DA, Benowitz NL. Risks and benefits of nicotine to aid smoking cessation in pregnancy. Drug Saf 2001;24(4):277–322. [PubMed: 11330657]
72. Akhter MP, Iwaniec UT, Haynatzki GR, Fung YK, Cullen DM, Recker RR. Effects of nicotine on bone mass and strength in aged female rats. J Orthop Res 2003;21:14–9. [PubMed: 12507575]
73. Silcox DH III, Daftari T, Boden SD, Schimandle JH, Hutton WC, Whitesides TE Jr. The effect of nicotine on spinal fusion. Spine 1995;20:1549–53. [PubMed: 7570168]
74. Fung YK, Mendlik MG, Haven MC, Akhter MP, Kimmel DB. Short-term effects of nicotine on bone and calciotropic hormones in adult female rats. Pharmacol Toxicol 1998;82:243–49. [PubMed: 9646330]
75. Iwaniec UT, Fung YK, Cullen DM, Akhter MA, Haven MC, Schmid M. Effects of nicotine on bone and calciotropic hormones in growing female rats. Calcif Tissue Int 2000;67:68–74. [PubMed: 10908416]
76. Iwaniec UT, Fung YK, Akhter MA, Haven MC, Nespor S, Haynatzki GR, Cullen DM. Effects of nicotine on bone mass, turnover, and strength in adult female rats. Calcif Tissue Int 2001;68:358–64. [PubMed: 11685424]

Author Manuscript Author Manuscript Author Manuscript Author Manuscript

77. Cesar-Neto JB, Duarte PM, Sallum EA, Barbieri D, Moreno H Jr, Nociti FH Jr. A comparative study on the effect of nicotine administration and cigarette smoke inhalation on bone healing around titanium implants. J Periodontol 2003;74:1454–59. [PubMed: 14653391]

78. Song MA, Marian C, Brasky TM, Reisinger S, Djordjevic M, Shields PG. Chemical and toxicological characteristics of conventional and low-TSNA moist snuff tobacco products. Toxicol Lett 2016;245:68–77. [PubMed: 26802282]

79. Hoffmann D, Adams JD. Carcinogenic tobacco-specific N-nitrosamines in snuff and in the saliva of snuff dippers. Cancer Res 1981;41(11 Pt 1):4305–8. [PubMed: 7198005]

80. Yalcin E, de la Monte S. Tobacco nitrosamines as culprits in disease: mechanisms reviewed. J Physiol Biochem 2016;72(1):107–20. [PubMed: 26767836]

81. Stepanov I, Hecht SS. Tobacco-specific nitrosamines and their pyridine-N-glucuronides in the urine of smokers and smokeless tobacco users. Cancer Epidemiol Biomarkers Prev 2005 4;14(4): 885–91. [PubMed: 15824160]

82. Kavvadias D, Scherer G, Cheung F, Errington G, Shepperd J, McEwan M. Determination of tobacco-specific N-nitrosamines in urine of smokers and non-smokers. Biomarkers 2009 12;14(8): 547–53. [PubMed: 19747086]

Author Manuscript Author Manuscript Author Manuscript Author Manuscript

- Snus adversely affects human embryonic stem cell calcification yield
- A video-based calcification analysis revealed delayed calcification kinetics
- Nicotine is not a major contributor to the osteotoxic effect of Snus
- NNN inhibited osteoblast differentiation at concentrations present in Snus
- NNN caused delayed calcification similar to that found with Snus

Author Manuscript Author Manuscript Author Manuscript Author Manuscript

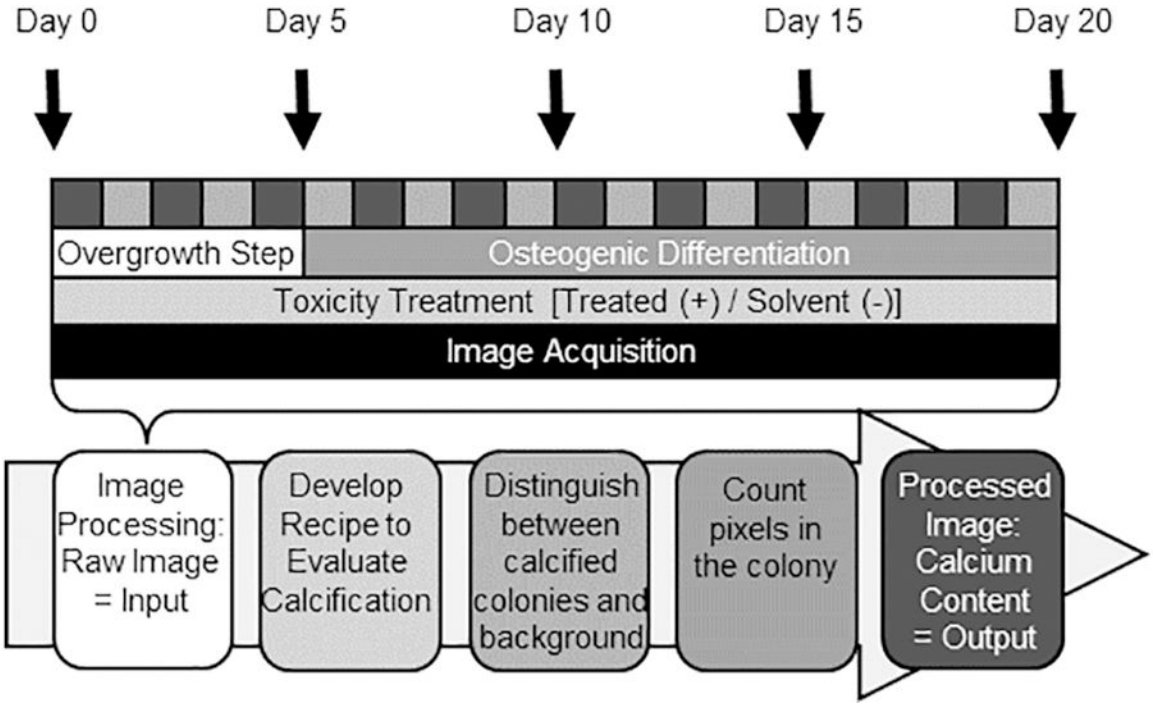


**Fig. 1. Schematic overview of image acquisition and data processing for video bioinformatic measurement of calcification.**

Cells are induced to undergo osteogenic differentiation through an overgrowth approach followed by addition of osteogenic factors on day 5. Differentiation is captured by time-lapse imaging every 12h for a period of 20 days using the Nikon Biostation CT. Time-lapse images are preprocessed to minimize noise from images. Calcification from images is segmented via manual threshold of pixel value set at 33 using MatLab. Numbers of segmented pixels representing calcified regions are quantified representing the amount of calcification from each time point of the time-lapse imaging.

Author Manuscript Author Manuscript Author Manuscript Author Manuscript

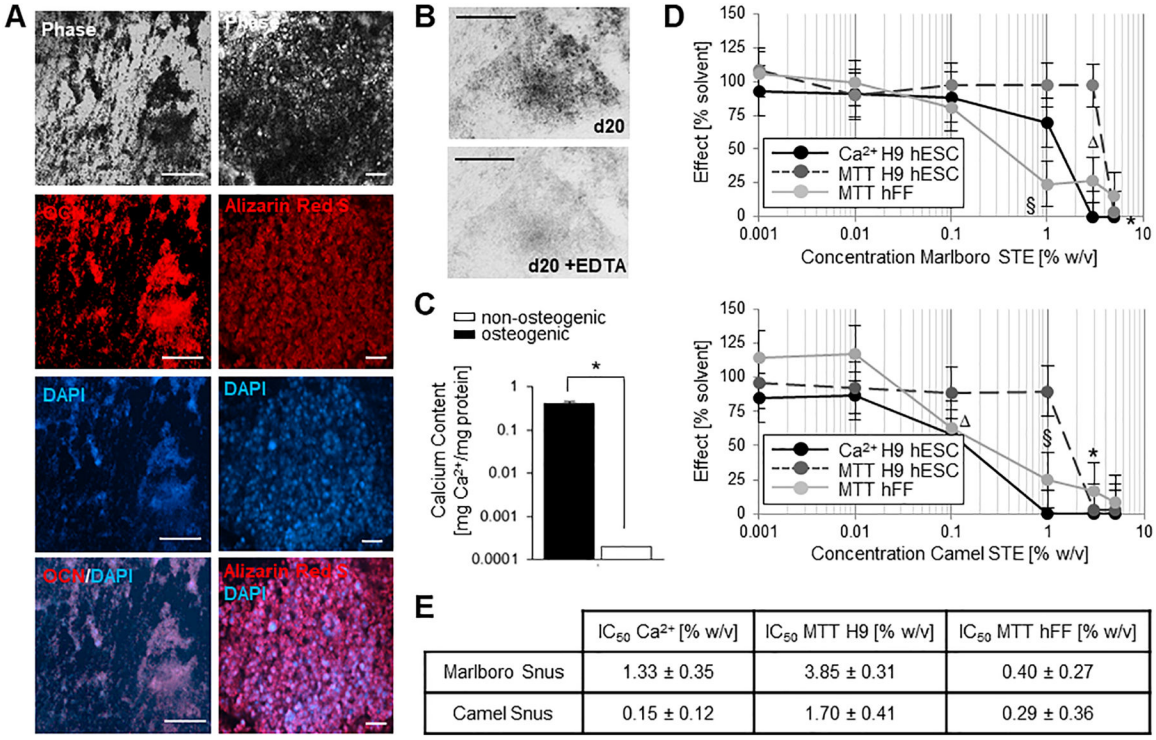


| | $IC_{50}$ $Ca^{2+}$ [% w/v] | $IC_{50}$ MTT H9 [% w/v] | $IC_{50}$ MTT hFF [% w/v] |
|---|---|---|---|
| Marlboro Snus | 1.33 ± 0.35 | 3.85 ± 0.31 | 0.40 ± 0.27 |
| Camel Snus | 0.15 ± 0.12 | 1.70 ± 0.41 | 0.29 ± 0.36 |

**Fig. 2. Osteogenic differentiation and calcification in human ESCs as endpoint for tobacco extract toxicity.**

(A) Osteogenic differentiation of human ESCs (H9 line) was confirmed on day 20 after differentiation induction by immunocytochemistry of the bone matrix marker osteocalcin (OCN) and deposited calcium ions visualized by Alizarin Red S staining. Bar = 20 μm. (B) Calcification was removable with 0.5 M EDTA. Bar = 100 μm. (C) Determination of calcium content in d20 cultures with Arsenazo III reagent, n=5 ± SD. **P*<0.05, student's t-test. (D) Concentration-response curves for cytotoxicity and differentiation inhibition (d20); n=5±SD. $^{\Delta}P$<0.05 = lowest concentration significantly below the solvent control in the Arsenazo III reagent-based calcium assay determined by One-Way ANOVA. **P*<0.05 = lowest concentration significantly below the solvent control in the MTT assay on H9 hESCs determined by One-Way ANOVA. $^{\S}P$<0.05 = lowest concentration significantly below the solvent control in the MTT assay on hFFs determined by One-Way ANOVA. (E) Summary of half-maximal inhibitory concentrations from concentration-response curves in (D). DAPI, 4',6-diamidino-2-phenylindole; hFF, human foreskin fibroblast; hESC, human embryonic stem cell; MTT, mitochondrial dehydrogenase activity assay; STE, Snus tobacco extract; OCN, osteocalcin.

Author Manuscript Author Manuscript Author Manuscript Author Manuscript

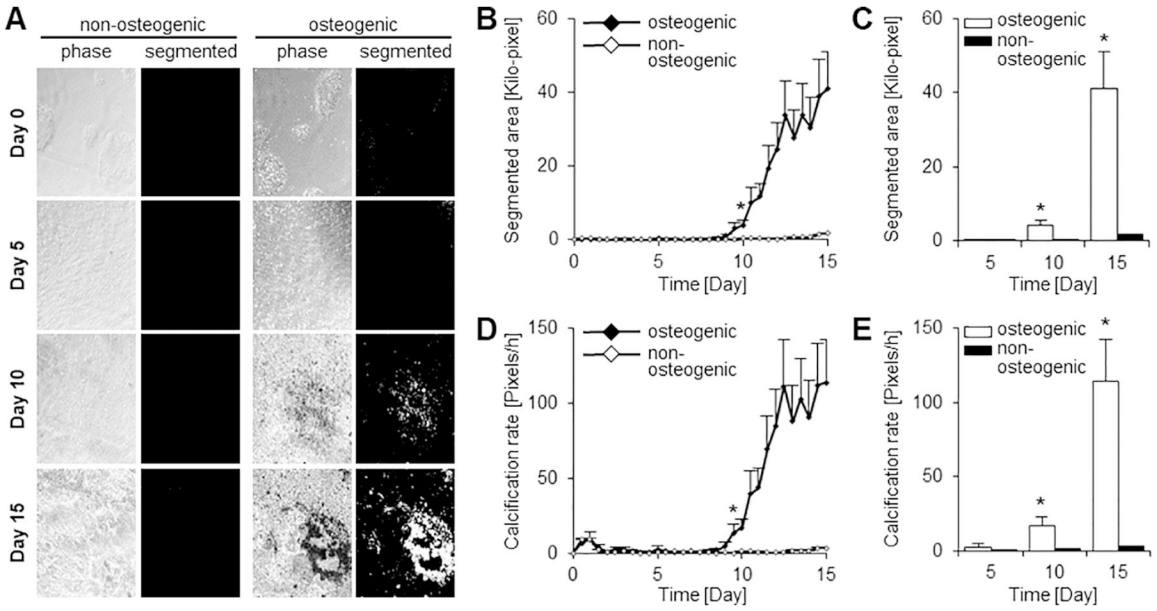


**Fig. 3. Determination of earliest measurable difference in calcification yield as endpoint for toxicity assessment.**

(A) Detection of calcified areas in images from osteogenic hESC cultures based on segmentation of pixels with a value of ≤33. (B, C) Calcium content of differentiating hESCs measured at 12h intervals from live cultures (B) and at specific days of the differentiation period (C). (D, E) Calcification rate based on the amount of calcification added in a given hour. (B-E) n=3 biological replicates (10 technical replicates ea) ± SD, **P*<0.05, One Way ANOVA versus the non-osteogenic condition; all subsequent days also exhibit a P value smaller than 0.05. STE, Snus tobacco extract.

Author Manuscript Author Manuscript Author Manuscript Author Manuscript

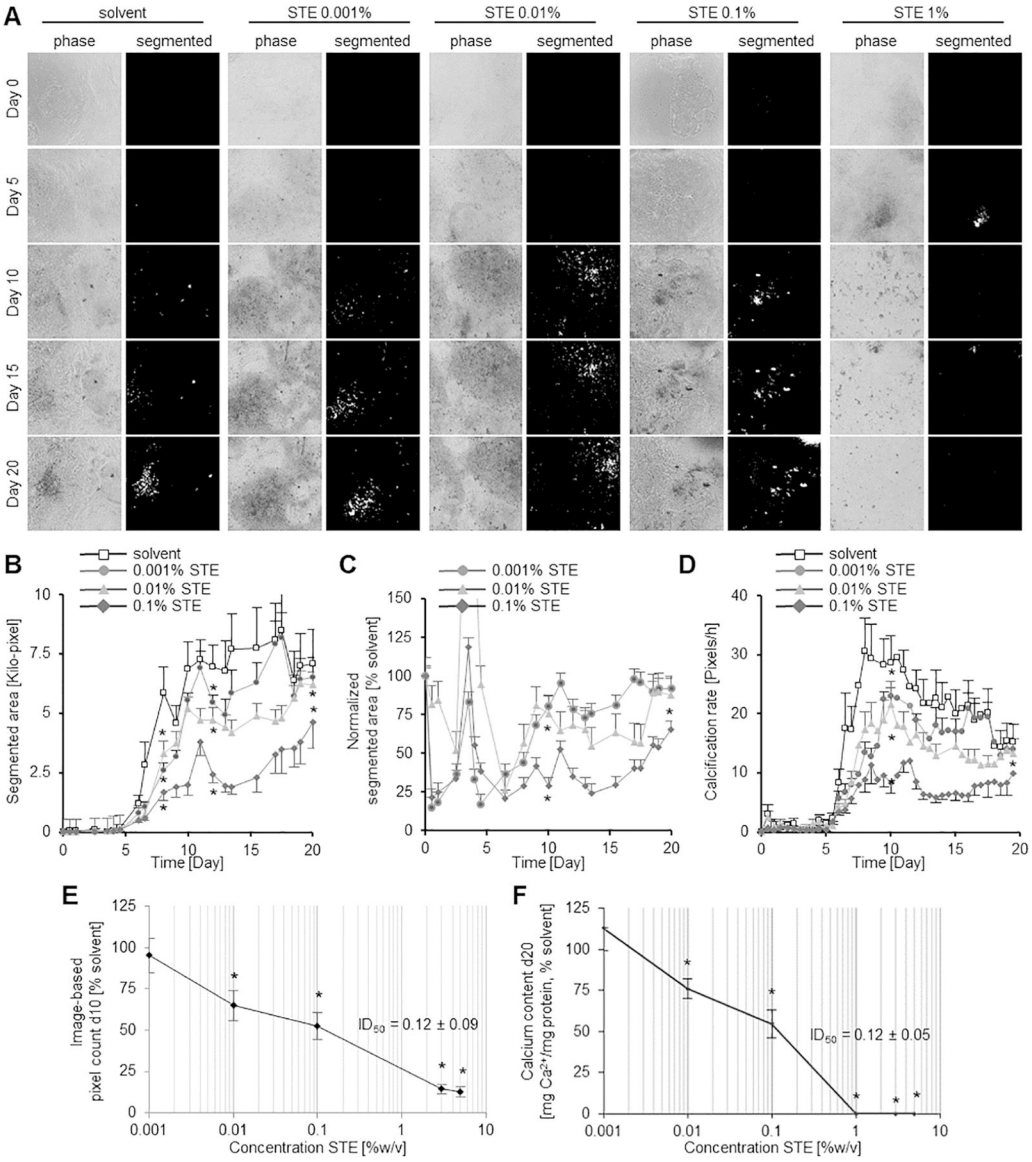


**Fig. 4. Video bioinformatics-based detection of calcification in hESC cultures treated with Camel Snus tobacco extract (STE).**

(A) Images show a decrease in the amount of calcification observed at 0.1% STE and cell death at 1% STE. (B) Image-based calcification was measured every 12h. (C) Normalized image-based calcification data. (D) Calcification rate calculated from images of tobacco treated samples. (B-D) show selected concentrations only for ease of readability. (E, F) Full concentration-response curves determined for all tested concentrations from 10-day-old cultures using video bioinformatics on segmented pixels and from d20 cultures using an Arsenazo III-reagent-based calcium assay. B-E n=3 biological replicates 10 technical replicates ea; F n=3, 5 technical replicates ea ± SD. *$P$<0.05, One Way ANOVA versus untreated. Statistics shown only for d10 and d20 for ease of readability. STE, Snus tobacco extract.

Author Manuscript Author Manuscript Author Manuscript Author Manuscript

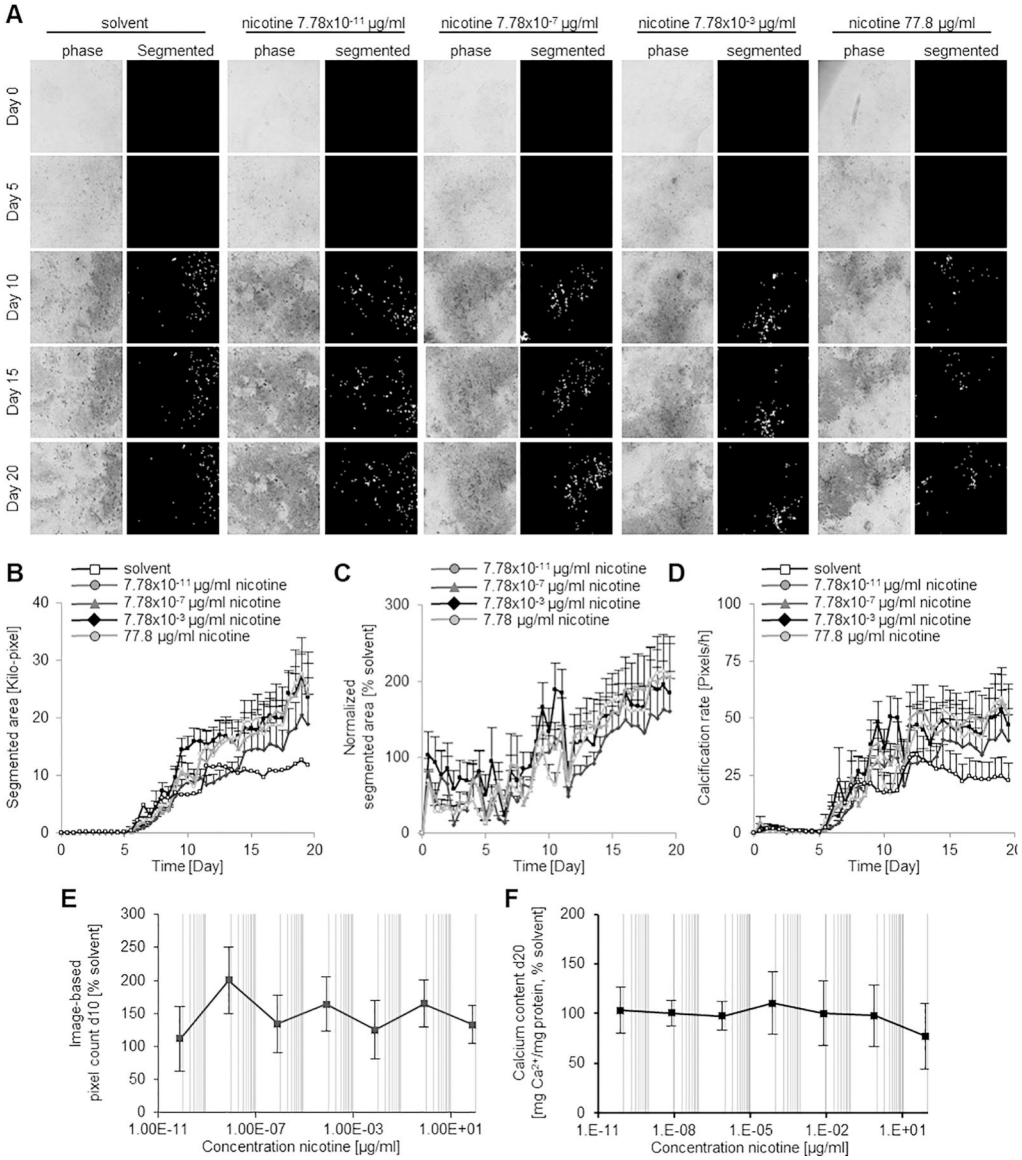


**Fig. 5. Video bioinformatics time-lapse images and calcium segmentation to study effects of nicotine on hESC osteogenesis.**

(A) No detrimental effects of nicotine on culture morphology could be detected in photomicrographs of cultures in the tested range. (B) Time-course calcification of nicotine treated osteogenically differentiating hESCs as shown every 12 hours. (C) Segmented areas in images of nicotine treated samples normalized to the solvent control. (D) Calcification rates of representative concentrations determined from images taken at 12h intervals. (B-D) show selected concentrations only for ease of readability. (E) Concentration-response calcification curve across all tested concentrations generated using image-quantified calcium measurement. (F) Arsenazo III reagent-based endpoint calcification curve. B-E n=3 biological replicates 10 technical replicates ea; F n=3, 5 technical replicates ea ± SD. **P*<0.05, One Way ANOVA versus untreated. Statistics shown only for d10 and d20 for ease of readability.

Author Manuscript Author Manuscript Author Manuscript Author Manuscript

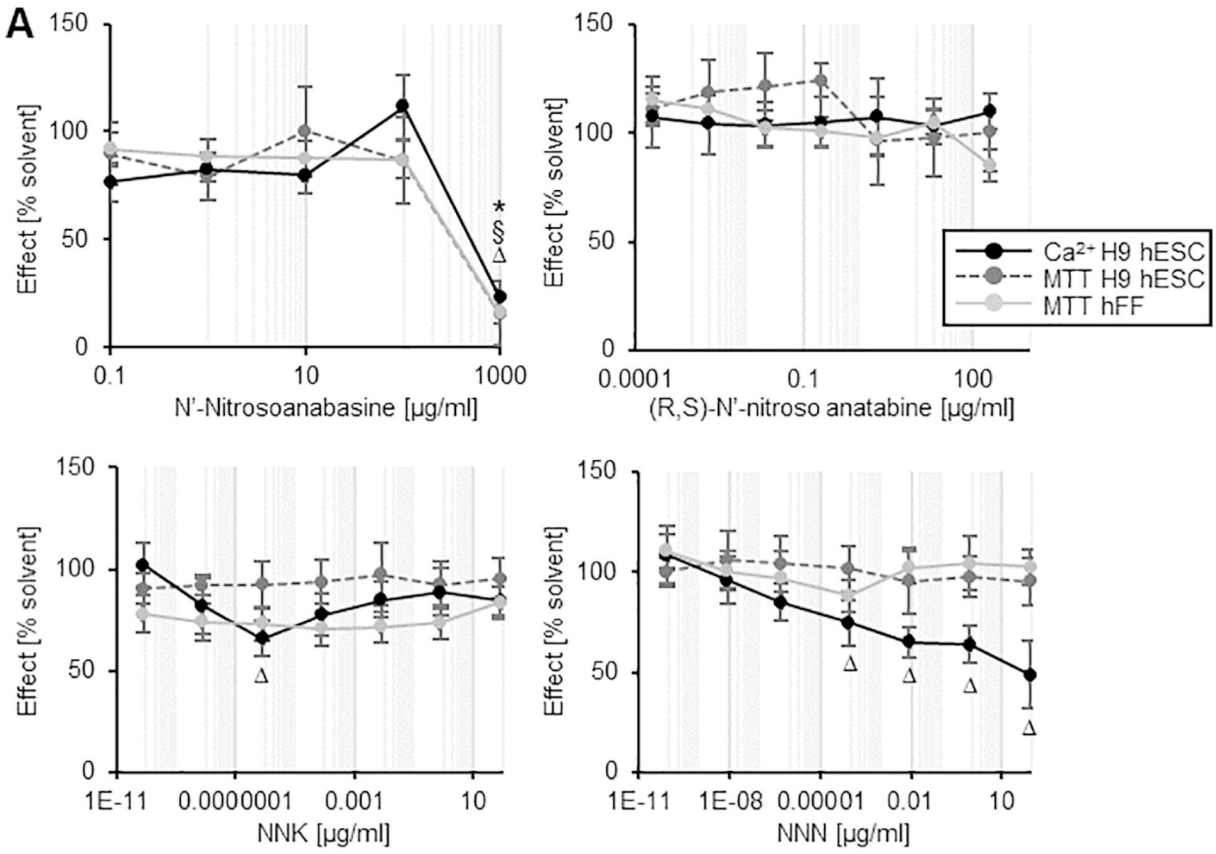


B

| | $IC_{50}$ $Ca^{2+}$ [µg/ml] | $IC_{50}$ MTT H9 [µg/ml] | $IC_{50}$ MTT hFF [µg/ml] | Concentration in STE [µg/mL] |
|---|---|---|---|---|
| NAB | 490 ± 165.2 | 315 ± 87.6 | 317 ± 130.1 | 0.00436±0.00011 |
| NAT | >200 | >200 | >200 | <0.02 |
| NNK | >18.9 | >18.9 | >18.9 | 0.0173±0.0004 |
| NNN | 8.55 ± 5.62 | >85 | >85 | 0.0618±0.0014 |

**Fig. 6. Cytotoxicity and differentiation inhibition caused by TSNAs.**

(A) Differentiation inhibition was measured by Arsenazo III reagent-based calcium assay on d20 of differentiation and contrasted to the cytotoxicity of the chemical in H9 hESCs and human foreskin fibroblasts also measured on d20. Values were calculated as percentage of solvent control and represent n=5±SD. $^{\Delta}P<0.05$, One-Way ANOVA versus solvent control in the Arsenazo III reagent-based calcium assay. $^{*}P<0.05$, One-Way ANOVA versus solvent control in the MTT assay on H9 hESCs. $^{\S}P<0.05$, One-Way ANOVA versus solvent control in the MTT assay on hFFs. (B) Table denoting half-maximal inhibitory concentrations deduced from graphical interpolation of data shown in (A) and listing of TSNA concentrations determined by HPLC analysis. hFF, human foreskin fibroblast; hESC, human embryonic stem cell; MTT, mitochondrial dehydrogenase activity assay.

Author Manuscript Author Manuscript Author Manuscript Author Manuscript

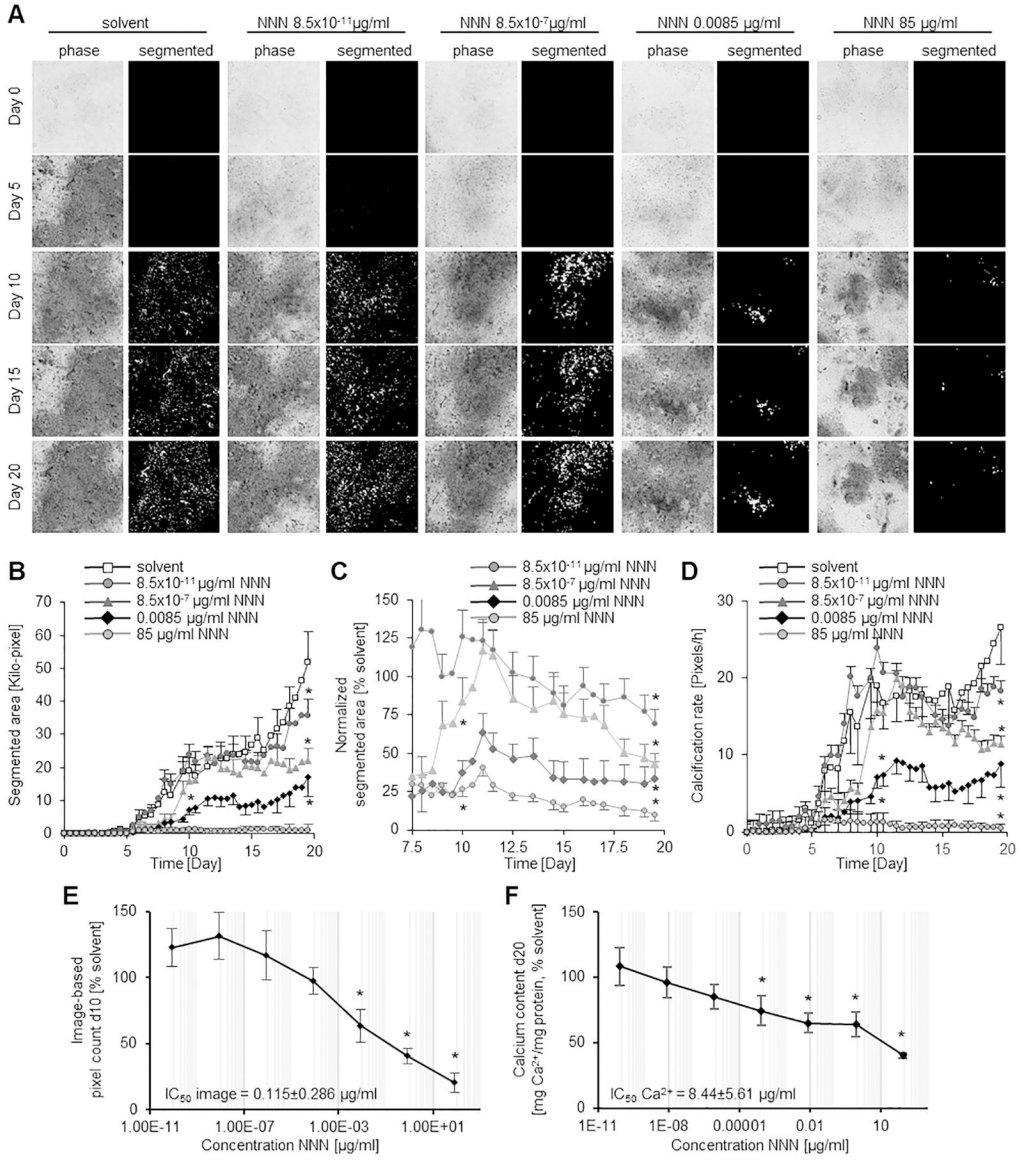


**Fig. 7. Video bioinformatic based detection of calcification in hESC cultures treated with N'-nitrosonornicotine (NNN).**

(A) Images show a decrease in the amount of calcification with higher concentration of NNN. (B) Image-based calcification was measured every 12h. (C) Normalized image-based calcification data. (D) Calcification rate calculated from images of NNN treated samples. (B-D) show selected concentrations only for ease of readability. (E) Concentration-response curve determined from 10-day-old cultures using video bioinformatics on segmented pixels, n=3 biological replicates (10 technical replicates ea) ±SD. **P*<0.05, One Way ANOVA versus untreated. (F) Concentration-response curve from d20 cultures using an Arsenazo III reagent-based calcium assay, n=3 ± SD. **P*<0.05, One Way ANOVA versus untreated. Statistics shown only for d10 and d20 for ease of readability.